

## Perspective

## Enhancing Exciton Diffusion Length Provides New Opportunities for Organic Photovoltaics

Muhammad T. Sajjad,<sup>1,2,\*</sup> Arvydas Ruseckas,<sup>1</sup> and Ifor D.W. Samuel<sup>1,\*</sup>

Organic semiconductors can potentially revolutionize solar cell technology by offering very thin, lightweight, and flexible modules for outdoor and indoor power generation. Light absorption in organic semiconductors generates a bound electron-hole pair (exciton), which needs to travel to the interface between electron donor and acceptor materials to dissociate into charge carriers. Because the exciton diffusion length in organic semiconductors is typically much shorter than the light absorption depth ( $\sim 100$  nm), planar donor-acceptor heterojunctions are inefficient, and most effort has been dedicated to optimization of bulk heterojunctions with nanoscale phase separation. In this Perspective, we review recent findings and new approaches to increase the exciton diffusion length and discuss how these improvements can benefit environmentally friendly production of solar modules using organic nanoparticles or graded heterojunctions obtained by sequential deposition of electron donor and acceptor.

## INTRODUCTION

Solar power is abundant and clean, making it a very promising renewable energy technology. Organic semiconductors have a range of attractive properties for photovoltaic applications, including high absorption coefficient so that the incident light can be absorbed in layers of thickness of  $\sim 100$  nm. Companies are already producing prototypes of lightweight and flexible solar modules and have installed large-area demonstrators for outdoor and indoor power generation. For example, 500 m<sup>2</sup> of solar films produced by the German company Heliatek were installed on the roof of a middle school in La Rochelle, France in 2017. These films weigh only 1 kg m<sup>-2</sup>, which is less than 5% of traditional solar modules, and are projected to provide about 15% of the school's electricity demand.<sup>1</sup> Heliatek films are deposited from the gas phase in low-pressure evaporators and laser patterned for optimal use of the available surface. Lower cost and higher volume manufacturing can potentially be achieved by solution processing (e.g., ink-jet printing or spray-coating) at (or near) room temperature.<sup>2</sup> Such procedures would also reduce the energy of manufacture. However, several problems need to be solved to realize this vision of widespread solution-processed organic photovoltaics.

Organic solar cells are typically made with an active layer sandwiched between transparent and reflecting electrodes (Figure 1). Absorption of light in the active layer generates a bound electron-hole pair called an exciton. To generate charge carriers, the exciton has to travel to the interface between electron donor and acceptor materials (heterojunction) where it can dissociate into a charge pair.<sup>3</sup> These pairs have to dissociate into free charge carriers and then be extracted to the electrodes to produce photocurrent. The two processes through which excitons can reach the heterojunction are direct Förster resonance energy transfer (FRET) between electron

## Progress and Potential

Organic photovoltaic solar cells (OPVs) have made remarkable progress, with lightweight and flexible solar modules now becoming commercially available and the first large-area installations completed. So far, these modules are produced by thermal evaporation in vacuum, which is an expensive technology. There is great potential for low-cost manufacture of OPVs by roll-to-roll coating of solution-processed materials, and efficient small cells have been reported using the bulk heterojunction architecture in which electron donors and acceptors are mixed on the nanoscale to enable charge generation in materials with short exciton diffusion length. However, the fabrication of such structures is delicate and difficult to scale up. Recent work shows that exciton diffusion length can be improved to enable exciton harvesting over longer distances, opening a pathway to much simpler manufacturing. In particular, enhanced exciton diffusion can improve light harvesting in solar cells that can be manufactured using water-based solutions of electron donor and acceptor nanoparticles or by sequential deposition of donor and acceptor, offering low-cost and environmentally friendly production.



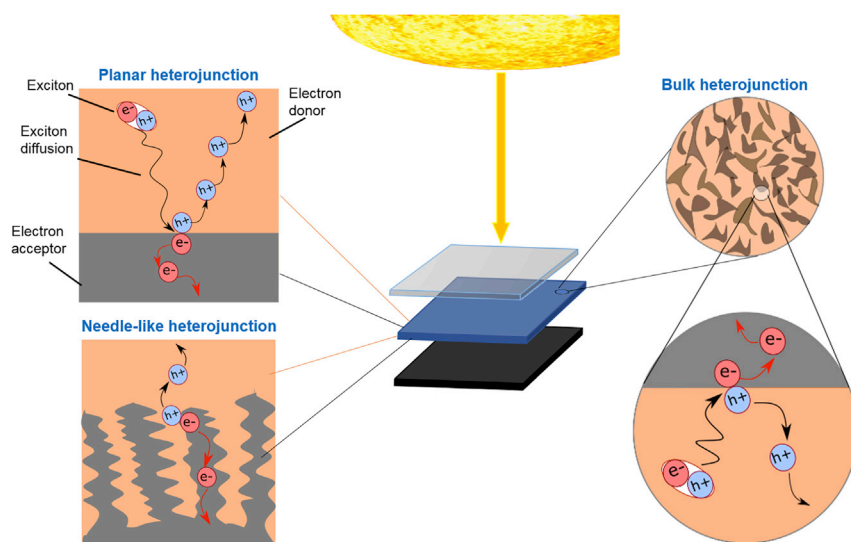


**Figure 1. Schematic of OPV Solar Cell with Three Different Morphologies of the Active Layer Sandwiched between a Transparent and Reflecting Electrode**

Different colors represent electron donor and acceptor materials. Excitons generated by light absorption in a donor or acceptor have to be transported to the interface between donor and acceptor where they can dissociate into free charge carriers. Only the excitons generated within their diffusion length  $L_D$  of the interface can contribute to photocurrent, therefore,  $L_D$  defines the useful thickness of donor and acceptor layers in planar heterojunctions and the acceptable length scale of phase separation in bulk and needle-like heterojunctions.

donor and acceptor, and diffusion. The distance that excitons can travel in their lifetime is called the exciton diffusion length ( $L_D$ ).

The simplest structure of the active layer is a bilayer of electron donor and acceptor, which makes a planar heterojunction (Figure 1). These structures are simple to make but suffer from a serious problem, namely the light absorption depth ( $\sim 100$  nm) is much longer than the exciton diffusion length.<sup>4–9</sup> This restricts the useful thickness of electron donor and acceptor layers, meaning that light is absorbed all the way through the donor layer, but only excitons created within  $L_D$  of the interface contribute to charge generation and, hence, photocurrent. This problem led researchers to make alternative device architectures by blending the electron donor and electron acceptor materials together to form a bulk heterojunction (BHJ) by phase separation. A BHJ does enable efficient charge generation and in the best cases has enabled small devices with efficiencies of 15%–17%.<sup>10–12</sup> However, charge extraction from such structures requires very precise control over the morphology, otherwise the large interface area between donor and acceptor can lead to significant charge recombination losses. The precise morphology requirement makes fabrication very delicate and represents a challenge for reliable large-scale manufacturing. Finding ways of increasing both  $L_D$  and domain sizes would simplify the structures, which would be easier to reproduce. The ideal structure of the active layer would be a needle-like heterojunction with well-defined charge generation and extraction pathways that could be optimized independently.

Another challenge is to produce suitable inks based on non-toxic and non-polluting solvents, preferably water as the cheapest and least harmful solvent. Currently the only component which is readily processed from aqueous solution is a hole-transporting polymer, PEDOT:PSS, while the morphology of charge generation layers

<sup>1</sup>Organic Semiconductor Centre, SUPA, School of Physics & Astronomy, North Haugh, St. Andrews KY16 9SS, UK

<sup>2</sup>Present address: London Centre for Energy Engineering, School of Engineering, London South Bank University, 103 Borough Road, London SE1 0AA, UK

\*Correspondence: [sajjad@lsbu.ac.uk](mailto:sajjad@lsbu.ac.uk) (M.T.S.), [ldws@st-andrews.ac.uk](mailto:ldws@st-andrews.ac.uk) (I.D.W.S.)

<https://doi.org/10.1016/j.matt.2020.06.028>

is usually optimized using chlorinated solvents. However, chlorinated solvents are not suitable for large-scale manufacturing processes, so alternatives based on less harmful green solvents are sought. Substantial effort has been directed to develop nanoparticulate organic photovoltaics (NP-OPVs), which use deposition of the active layer from water-based solutions.<sup>13–15</sup> So far the efficiencies of NP-OPVs are much lower than those of BHJs, and recent studies showed that exciton harvesting is a limiting process. For example, solar cells made from nanoparticles of poly(3-hexylthiophene) (P3HT) blended with nanoparticles of an electron acceptor, PCBM, absorbed about 90% of photons in the region from 400 to 600 nm. However, the external quantum efficiency (EQE) was only 20%.<sup>15</sup> This can be explained by the fact that  $L_D$  (~10 nm) in P3HT<sup>16</sup> is much shorter than the typical particle size (~40 nm). Hence, increasing  $L_D$  is very important for the development of future NP-OPVs.

In this Perspective, we briefly describe the main techniques to measure exciton diffusion length and their applicability. We then review some successful approaches that have led to increased exciton diffusion length in OPV materials and better device performance. Finally, we discuss possible ways to further enhance exciton diffusion and how it can be used in environmentally friendly production of flexible and light-weight solar cells.

## TECHNIQUES TO MEASURE EXCITON DIFFUSION

The exciton motion by a random walk can be quantified by the exciton diffusion coefficient  $D$ , which could be isotropic or anisotropic. In the literature it is common to define the average exciton diffusion length as  $L_{ZD} = \sqrt{ZD\tau}$ , where  $D$  is the effective diffusion coefficient,  $\tau$  is the exciton lifetime and  $Z$  is the dimensionality of diffusion, which is equal to 1, 2, or 3 for one-dimensional (1D), two-dimensional (2D), or three-dimensional (3D) diffusion, respectively,<sup>5</sup> although some researchers include an additional factor 2 in the square root. Various techniques have been used to measure exciton diffusion, each with advantages and disadvantages. These include measurements of photoluminescence quenching (steady-state and time-resolved), direct imaging of exciton diffusion, transient microwave conductivity, transient absorption spectroscopy, and measurements of internal quantum efficiency (IQE) or photovoltage in planar heterojunctions. These techniques have been described in detail in previous reviews,<sup>5–7</sup> so in this Perspective we briefly discuss the main requirements and applicability of the techniques.

Surface quenching of photoluminescence (PL) is a simple and reliable technique to measure exciton diffusion. For this, a film of the studied material is deposited on the top of a quencher and steady-state or time-resolved PL quenching is measured.  $D$  is then extracted from the dependence of PL quenching on film thickness. The advantage of this technique is that it measures exciton diffusion in bilayer structures and is directly linked to planar heterojunction photovoltaics. Time-resolved PL quenching gives more data and therefore constrains fits more than steady-state measurements, and also avoids some drawbacks of steady-state measurements, including the dependence on optical geometry.<sup>17</sup> The technique requires an effective quencher that does not mix with or penetrate the test material. For example, using fullerene as a quencher deposited on top of the organic semiconductor leads to diffusion of fullerene molecules into the organic layer, higher PL quenching and, thus, overestimation of diffusion length.<sup>18</sup> This problem of interdiffusion can be overcome by either crosslinking<sup>8,9,18,19</sup> or tethering<sup>20</sup> the fullerene derivatives to the substrate. Furthermore, in the event that the fluorescence spectrum of the

studied material overlaps with the absorption spectrum of the quencher, long-range FRET to the quencher can occur, which should be included in the analysis.

Volume quenching of PL is a popular technique to measure exciton diffusion whereby a small known quantity of the quencher is dispersed in a donor material and PL quenching is measured as a function of quencher concentration.  $D$  is extracted by fitting experimental data using either the Smoluchowski equation or Monte Carlo simulation. Stern-Volmer analysis can be used in the case of monoexponential PL decays. Volume quenching measures the 3D exciton diffusion and requires a homogeneous dispersion of the quencher. This technique is not suitable for semicrystalline materials because excitons diffuse into crystalline domains where their energy is lower, while the quencher is expelled from these domains. This leads to much weaker PL quenching and underestimation of  $D$ . Even for amorphous materials, this technique has to be used with caution using only low concentration of the quencher dispersed throughout the film because quenchers at higher concentration often form clusters. A range of quencher concentrations has to be investigated to establish the cluster-free regime. For example, Ward et al. found that in amorphous material the quencher (fullerene) concentration should not exceed  $0.007 \text{ nm}^{-3}$  to avoid clustering.<sup>20</sup> It is also important that quenching occurs on the first encounter with a quencher, which requires a fast energy or electron transfer to the quencher. For example, it was shown that the electron transfer rate from the conjugated polymer PTB7 to dispersed fullerene electron acceptor molecules depends on the offset of energy levels (driving force), and the fastest rate was observed for the offset of  $\sim 0.4 \text{ eV}$ .<sup>21</sup> Long-range FRET should also be included in the analysis when relevant.

Exciton-exciton annihilation can provide information on the dimensionality of diffusion as well as  $D$  values. In this method, one exciton acts as a quencher for another exciton. This process occurs at high excitation densities when two excitons are close enough so that one of them transfers its energy onto the other, forming a higher energy exciton which then cools down. Usually, one exciton is lost per annihilation event. The PL decays are measured at different initial excitation densities so that the annihilation rate constant and exciton diffusivity are deduced by modeling these decays. For this technique, it is important to measure annihilation-free decay at very low excitation density in the studied material as a reference. The advantages of this technique are that it requires only one sample to measure exciton diffusion, and therefore is very useful to evaluate the effect of a wide range of processing conditions on exciton diffusion. Exciton-exciton annihilation involves both exciton diffusion and direct FRET from one exciton to the other; therefore, both time-dependent and time-independent terms should be included in the analysis. The time-dependent term gives information about the dimensionality of the diffusion and in some cases can be used to estimate the annihilation radius  $R_a$ . Shaw et al. used two complementary techniques of PL surface quenching and exciton-exciton annihilation to measure  $D$  and  $R_a$  independently in P3HT.<sup>16</sup> Zhang et al.<sup>8</sup> and Long et al.<sup>19</sup> used the value of  $d_{100}$ -spacing determined by X-ray diffraction studies for  $R_a$  and obtained good agreement with PL surface-quenching measurements.

The diffusion length of non-emissive excitons is more difficult to determine and usually has been estimated from the photocurrent action spectrum in planar heterojunction solar cells by combining it with an optical model to describe the electric field distribution in the active layer, which determines the spatial profile of photogenerated excitons.<sup>22–24</sup> This method has to make assumptions about the efficiency of charge pair dissociation into free carriers and extraction from the device under short-circuit conditions. The assumption that all the charges generated at the

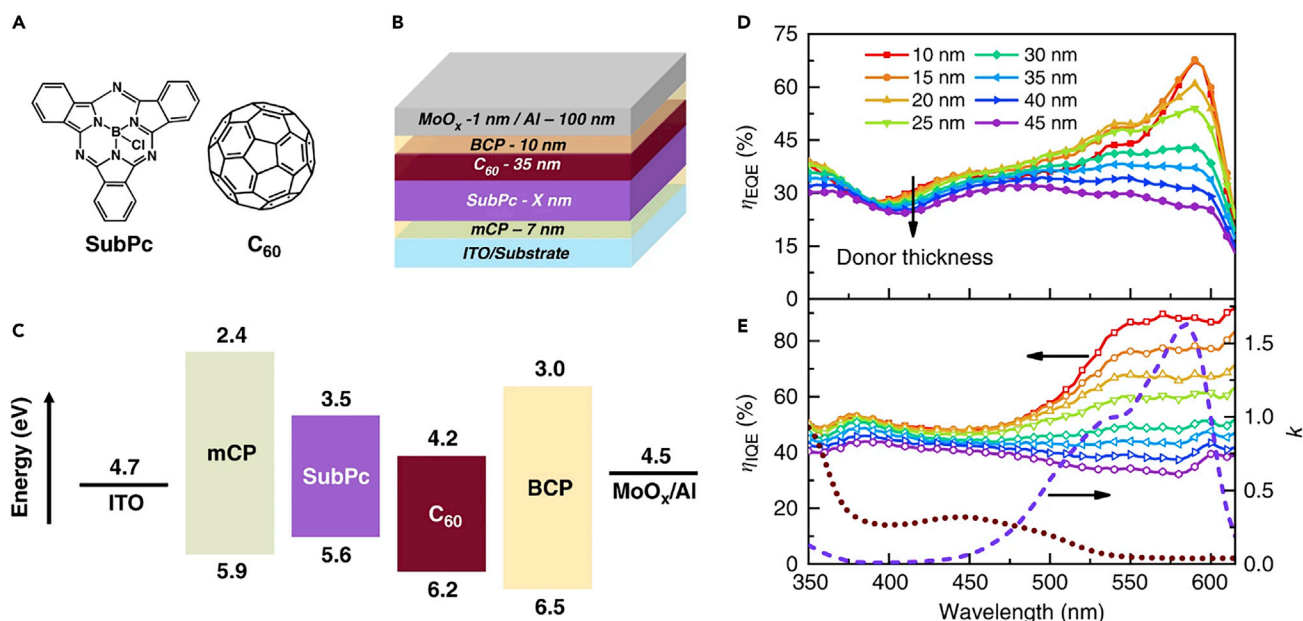


**Figure 2. Extracting Exciton Diffusion Length from the Ratio of Internal Quantum Efficiencies**

(A–C) Solar cell structure using planar heterojunction of SubPc and C<sub>60</sub> (A and B) and energy level diagram (C). (D) The external quantum efficiency (EQE) spectra measured at short-circuit as a function of SubPc layer thickness. (E) The internal quantum efficiency (IQE) spectra calculated by dividing the EQE spectra in (D) by the absorption efficiency calculated using a transfer matrix model. The extinction coefficients (*k*) of SubPc (purple dashed line) and C<sub>60</sub> (brown dotted line) are also shown. Reprinted from Zhang et al.<sup>27</sup> Licensed under CC-BY-3.0.

interface are extracted gives a lower bound of  $L_D$ . The uncertainty of free carrier collection can be overcome by measuring transient photovoltage; however, the determined  $L_D$  values in some cases were still lower than those by fluorescence quenching, which was attributed to geminate recombination losses.<sup>25</sup> Siegmund et al. proposed a method to determine the exciton diffusion length and the combined efficiency of charge pair dissociation and extraction  $\eta_c$  by varying the absorber thickness and modeling of photocurrent action spectra.<sup>26</sup> They obtained the 1D exciton diffusion length  $L_D \approx 10$  nm in zinc phthalocyanine (ZnPc) and  $\eta_c \approx 0.58$  in solar cells based on planar heterojunction of ZnPc and C<sub>60</sub>. The diffusion length value is in good agreement with fluorescence surface-quenching measurements. A later study showed that the uncertainty of geminate recombination losses is not critical when taking the ratio of IQEs measured in the donor and acceptor absorption regions (Figure 2).<sup>27</sup> Again, good agreement with fluorescence quenching measurements was obtained (values are given in Table 1).

## EFFECT OF DISORDER AND CRYSTALLINITY

Exciton diffusion in organic semiconductors occurs by hopping of excitons between chromophores. Organic layers used in OPVs can be fully amorphous or partially crystalline with ordered domains embedded in a disordered matrix. In amorphous materials each chromophore is in a slightly different environment from adjacent chromophores and sometimes has a different conformation too; hence, their excitation energies also differ. This energetic disorder is characterized by the width of the density of states (DOS)  $\sigma$  (Figure 3). The exciton generated within the DOS will hop predominantly to chromophores of lower energy until it reaches a site that has lower energy than the adjacent sites. This can be observed experimentally as a dynamic red-shift of fluorescence or stimulated emission and a decay of polarization

**Table 1. Exciton Diffusion Coefficient  $D$  and One-Dimensional Exciton Diffusion Length  $L_{1D}$  in Frequently Used OPV Materials**

Material	$D$ ( $10^{-3} \text{ cm}^2 \text{ s}^{-1}$ )	$L_{1D}$ (nm)	Measurement Technique
SubPc	–	$16.7 \pm 1.7$ $16.6 \pm 2.0$	IQE ratio PL surface quenching <sup>27</sup>
SubNc	–	$21.2 \pm 2.2$	IQE ratio <sup>27</sup>
C <sub>60</sub>	–	<b>18.5 or 21.3<sup>a</sup></b> $18.5 \pm 3.0$	IQE ratio <sup>27</sup> PL surface quenching <sup>27</sup>
C <sub>70</sub>	–	$7.4 \pm 0.8$	IQE ratio <sup>27</sup>
ZnPc	– $0.7 \pm 0.2$	$10.1 \pm 0.9$ $9.6 \pm 0.8$	IQE <sup>26</sup> PL surface quenching <sup>26</sup>
H2Pc neat H2Pc triplet-sensitized	–	$13.4 \pm 1.6$ $20.7 \pm 5.0$	IQE ratio <sup>28</sup>
P3HT	1.8 1–5 <sup>b</sup> 7.9	8.5 – 20	PL surface quenching <sup>16</sup> annihilation <sup>29</sup> annihilation <sup>6</sup>
P3HT-co-P3DDT	3.9 (SVA)	$6.7 \pm 0.7$ (SVA)	annihilation <sup>30</sup>
DTS(FBTTh <sub>2</sub> ) <sub>2</sub>	3.6 (TA)	13.5 (TA)	PL surface quenching <sup>19</sup>
PTB7	–	$4.5 \pm 0.5$	IQE ratio <sup>27</sup>
DR3TBDTT	4.5 (SVA)	18.4 (SVA)	PL surface quenching <sup>9</sup> annihilation <sup>31</sup>
SMPV1	1 (SVA)	5.7 (SVA)	annihilation <sup>31</sup>
BQR	5 (SVA)	17.5 (SVA)	annihilation <sup>32</sup>
BTR	4 (SVA)	16.3 (SVA)	annihilation <sup>32</sup>
PfBT4T-2OD	3 (TA)	17.0 (TA)	annihilation <sup>8</sup>
ANE-PVab	$0.59 \pm 0.06$	$6.2 \pm 0.3$	PL volume quenching <sup>33</sup>
PC <sub>71</sub> BM	0.16	3	PL volume quenching <sup>7</sup>
IDIC	20	16	annihilation <sup>34</sup>

The first six rows represent films deposited from the gas phase while the remaining 12 rows represent films coated from solution. For measurements where  $D$  is shown, the 1D diffusion length was determined using  $L_{1D} = \sqrt{D\tau}$ , where  $\tau$  is the exciton decay time. SVA is a film treatment by solvent vapor annealing and TA is thermal annealing.

<sup>a</sup>With different donor layers.

<sup>b</sup>For different molecular weights.

anisotropy, which usually occur on a timescale of a few picoseconds at room temperature.<sup>35–39</sup> Further hopping after this requires thermal activation or FRET to non-nearest neighbors; hence, the diffusion coefficient initially decreases and then reaches a thermal equilibrium value.<sup>40</sup> The energy distribution of excitons in thermal equilibrium is called the occupied density of states (ODOS). In the case of no structural relaxation in the excited state, the center of the ODOS is shifted by  $\sigma^2/kT$  to lower energy relative to the center of the DOS.<sup>41</sup> Lowering energetic disorder as well as preventing any structural relaxation in the excited state will bring ODOS and DOS closer in energy and provide more pathways for excitons to hop; hence, longer exciton diffusion is expected in materials with lower width of DOS (i.e., higher crystallinity).

Many studies showed that excitons can diffuse longer distances in materials with larger crystalline domains. For example, Lunt et al. reported a nearly 4-fold enhancement in 1D diffusion length from  $\sim 6$  nm to  $\sim 22$  nm for the archetypal organic semiconductor 3,4,9,10-perylene-tetracarboxylic dianhydride (PTCDA) through an increase in crystalline domain size from 100 to 400 nm.<sup>43</sup> They found that this increase in diffusion length is connected to an increase in the fluorescence quantum yield, suggesting that exciton

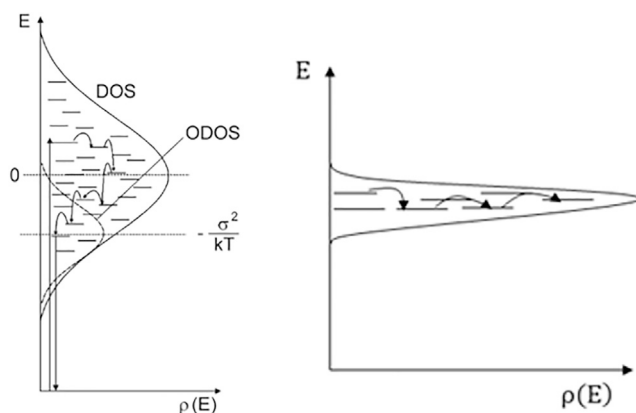


**Figure 3. Density of States Representing Distribution of Excitation Energies in Disordered Materials**

The exciton initially hops to the sites of lower energy until they quickly reach the equilibrium energy, which is offset by  $\sigma^2/kT$  with respect to the center of the density of states (DOS). Here  $\sigma$  is the half-width of the Gaussian energy distribution and  $kT$  is the thermal energy. For excitons at the equilibrium energy there are fewer available hopping sites, which slows down exciton diffusion. Reprinted with permission from Laquai et al.<sup>42</sup> The right-hand figure shows DOS with a narrow energy distribution in ordered materials where excitons have more nearest neighbors for nearly isoenergetic hopping.

diffusion length is limited by non-radiative decay at grain boundaries. Lin et al. studied exciton diffusion in a family of diketopyrrolopyrrole (DPP) derivatives with different conjugation lengths. They found that decreasing the conjugation length increases molecular ordering, which is correlated with an enhancement of 1D exciton diffusion length from 9 to 13 nm.<sup>44</sup> Li et al. carried out first-principles simulations of exciton diffusion in the same DPP derivatives and obtained good agreement with experiments as well as strong correlation between exciton diffusion length and ratio of crystalline-to-amorphous film volume.<sup>45</sup> Our group has also observed faster and longer exciton diffusion in more crystalline materials.<sup>19,30–33</sup>

In addition to reduced energetic disorder, other factors can cause longer exciton diffusion in crystalline materials, such as shorter intermolecular distances because of denser packing, better alignment of transition dipoles, and increased exciton lifetime. On the other hand, crystalline organic films usually have a higher surface roughness, which can be detrimental to charge extraction. A balance should be struck when optimizing different parameters in OPVs.

### INCREASING EXCITON DIFFUSION BY PROCESSING

Film crystallinity can be changed using thermal annealing. Sim et al. have shown that annealing P3HT film at 235°C increased 1D diffusion length from 3.3 to 7 nm.<sup>46</sup> Long et al. found a substantial increase of 2D  $L_D$  to  $\sim 27$  nm in a small electron donor molecule DTS-(FBTTh<sub>2</sub>)<sub>2</sub> upon thermal annealing at 130°C.<sup>19</sup> Zhang et al. showed that thermal annealing of the semiconducting polymer PffBT4T-2OD increases the crystallite size by  $\sim 40\%$ , which nearly doubled the 3D diffusion length to  $\sim 30$  nm.<sup>8</sup> They fabricated BHJ solar cells using this polymer with PC<sub>71</sub>BM as electron acceptor and obtained an enhancement of the power conversion efficiency (PCE) from 7.3% to 9.0% by thermal annealing at 100°C for 5 min.

In some cases, solvent vapor annealing (SVA) was found to be a more effective and reliable method to increase exciton diffusion length. In SVA, solvent vapors are used to swell



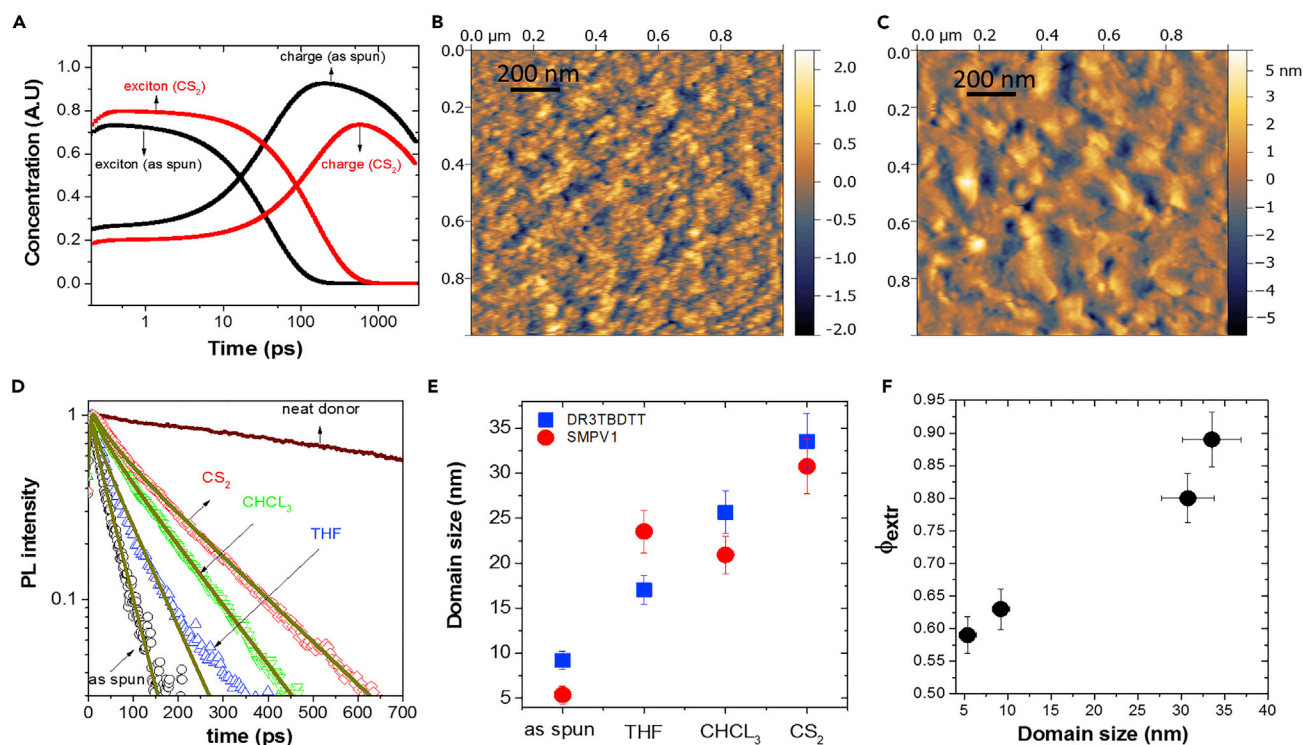


**Figure 4. The Effect of Processing on Domain Size and Charge Extraction Efficiency in BHJ of the Small Donor Molecule DR3TBDTT with PC<sub>71</sub>BM**

(A) Dynamics of charge generation obtained from transient absorption spectra before and after solvent vapor annealing (SVA). (B and C) AFM images of BHJ before (B) and after (C) SVA in carbon disulfide (CS<sub>2</sub>) showing larger length scale of phase separation after SVA. (D) Time-resolved PL quenching in as-spun blend and after SVA in different solvents. (E) Average domain sizes of PC<sub>71</sub>BM extracted from PL quenching data in as-spun blend and after SVA in different solvents. (F) Charge extraction efficiency as a function of average domain size.

Reprinted with permission from Sajjad et al.<sup>31</sup>

the film, thus allowing polymer rearrangement, which then increases the overall crystallinity of the film. For example, Chowdhury et al. observed a larger enhancement of the relative degree of crystallinity and exciton diffusion length by SVA with carbon disulfide (CS<sub>2</sub>) than for thermal annealing in a conjugated copolymer poly-(3-hexylthiophene-co-3-dodecylthiophene) (P3HT-co-P3DDT).<sup>30</sup> Wei et al. showed that SVA with dichloromethane increases  $L_D$  by a factor of 3 compared with thermal annealing in the squaraine derivative.<sup>47</sup> Thermal annealing and SVA have been reported to increase the 3D exciton diffusion length to about 40 nm in two liquid crystalline electron donor materials, BQR and BTR, which is almost twice as long as in cast films.<sup>32</sup> We also found a similar increase of  $L_D$  in the small-molecule electron donors DR3TBDTT and SMPV1 upon SVA, which enabled us to demonstrate charge extraction efficiency up to 90% at short-circuit conditions in blends with PC<sub>71</sub>BM (Figure 4).<sup>31</sup> This was achieved with relatively large domain sizes of ~30 nm, which still gave us efficient exciton harvesting due to the long diffusion length. This shows that SVA can be used to tailor exciton diffusion and domain size to optimize both charge generation and extraction.

## INTERLAYER FÖRSTER RESONANCE ENERGY TRANSFER

In contrast to diffusion, which involves a random walk in all directions, FRET between electron donor and acceptor materials is directional and can bring excitons directly to a heterojunction. It has a big advantage for applications in planar heterojunctions because of a favorable scaling of FRET rate with the distance  $R$  between layers (approximately  $R^{-3}$  versus  $R^{-6}$  in the case of energy transfer between single



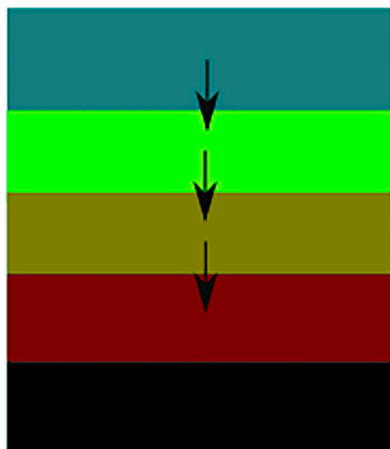


**Figure 5. Schematic of Energy Cascade Structure Designed to Direct Exciton Motion**

Here, the excitation energy of consecutive layers of materials is slightly lower than the previous layer to flow excitons “downhill” in energy.

chromophores).<sup>48,49</sup> Cnops et al. applied this strategy to fabricate three-layer devices using  $\alpha$ -sexithiophene ( $\alpha$ -6T) as electron donor, boron sub-naphthalocyanine chloride (SubNc) as an electron acceptor, and boron subphthalocyanine chloride (SubPc) as an additional light-harvesting interlayer.<sup>50</sup> The SubPc excitons are efficiently harvested through energy transfer to ( $\alpha$ -6T) followed by electron transfer to SubNc. They demonstrated an impressive PCE of 8.4% in a planar heterojunction device. Wang et al. have shown that the addition of the low-band-gap donor polymer PSBTBT into RR-P3HT/PCBM blends could double the effective 1D diffusion length of RR-P3HT from 15 to 30 nm.<sup>51</sup> Honda et al. have applied this strategy to ternary BHJ OPVs, whereby they incorporated silicon phthalocyanine as an additional light-harvesting dye into RR-P3HT/PCBM blends and showed an improvement in photocurrent density and PCE.<sup>52</sup>

The potential to design multilayer heterojunctions with a FRET energy cascade between layers has been explored by Reid and Rumbles using experimentally verified Monte Carlo simulations (Figure 5).<sup>53</sup> They showed that a PCE of 10% is plausible and 15% is theoretically possible, assuming a typical 0.6-eV energy loss at the heterojunction.

### INCREASING EXCITON LIFETIME

Exciton diffusion length is proportional to both square root of diffusion coefficient ( $D$ ) and square root of exciton lifetime ( $\tau$ ). Most work has focused on increasing the diffusion coefficient, but ways to increase lifetime have also been explored. Menke et al. diluted the electron donor boron sub-phthalocyanine chloride in a high-band-gap host material UGH2 and observed 6-fold enhancement in a lifetime from 0.5 to 3 ns. This increase in lifetime led to a ~43% increase in 1D diffusion length from 10.7 to 15.3 nm.<sup>54</sup> They then fabricated planar heterojunction solar cells using this approach with  $C_{60}$  as an electron acceptor and obtained a 30% higher PCE than control cells made using undiluted molecules. However, the opposite effect has also been observed whereby dilution of molecules decreases the exciton lifetime. For example, Caplins et al. observed a 3-fold decrease of exciton lifetime when they diluted metal-free phthalocyanine ( $H_2Pc$ ) in the same host UGH2, showing that chromophore density is not the only factor determining the exciton lifetime, specific intermolecular interactions also being involved.<sup>55</sup>

The exciton lifetime can be enhanced by converting singlet excitons to longer-lived triplet excitons. Shi et al. used a dopant molecule with fast intersystem crossing as

triplet sensitizer in H<sub>2</sub>Pc and increased  $L_{1D}$  to 13.4 nm.<sup>28</sup> They also measured a lower limit of the triplet diffusion length in neat H<sub>2</sub>Pc films of ~20 nm, which suggests that further enhancement of  $L_D$  may be possible with further optimization of the sensitization scheme.

## HETEROJUNCTIONS WITH NON-FULLERENE ACCEPTORS

Recently, big improvements in OPV efficiency and stability have been achieved using non-fullerene electron acceptors (NFAs) instead of fullerene derivatives.<sup>56</sup> Small solar cells with over 16% efficiencies have been reported using BHJs with NFAs in binary and ternary blends.<sup>11,57,58</sup> Resonant soft X-ray scattering measurements have indicated quite large donor and acceptor domains of 20–50 nm and high domain purity in BHJ with NFAs.<sup>59</sup> Efficient exciton dissociation observed in these BHJs implies that the exciton diffusion length is at least comparable with these domain sizes and is consistent with the observation of strong exciton-exciton annihilation reported in several fused-ring electron acceptors at excitation densities of 1  $\mu\text{J cm}^{-2}$  and higher.<sup>34</sup> These observations make exciton diffusion studies in NFAs an important direction for future exploration.

In recent years the sequential deposition of donor and acceptor layers has been successfully implemented to fabricate efficient (>10%) and more stable organic solar cells with up to 1 cm<sup>2</sup> surface area using NFAs.<sup>60–63</sup> These could be prepared using a pair of eco-friendly non-halogenated solvents, such as (*R*)-(+)-limonene (LM) and 2-methyltetrahydrofuran.<sup>64</sup> The vertical distribution of donor and acceptor molecules in sequentially deposited layers has been explored using STEM-EDX (cross-sectional scanning transmission electron microscopy-energy dispersive X-ray spectroscopy) and UV photoemission spectroscopy depth profiling.<sup>65</sup> Both techniques indicated gradual donor-acceptor composition change in the top half of the film and a uniform distribution in the bottom half. This suggests that sequential deposition of donor and acceptor produces a graded BHJ where the amount of mixing is controlled by the amount of the second solvent. This morphology is similar to a “needle-like” heterojunction schematically shown in Figure 1, which can provide efficient exciton harvesting with moderate exciton diffusion length and well-defined pathways for charge extraction. Enhanced exciton diffusion length opens new opportunities for morphology optimization using this approach.

## FUTURE OUTLOOK AND CONCLUSIONS

Long exciton diffusion length opens new opportunities for organic photovoltaic technologies. First it enables the use of larger donor and acceptor domain sizes in BHJs, which show benefits of more efficient charge pair dissociation and charge extraction. Long exciton diffusion length increases the tolerance of optimum morphology of BHJs and thus can reduce device degradation due to increasing phase separation. It also has the potential to boost the efficiencies of nanoparticulate OPVs, which offer environmentally friendly, low-cost production by ink-jet printing or sputtering of electron donor and acceptor nanoparticles from water-based solutions. The typical size of such nanoparticles is 40 nm and similar to the optimized 3D diffusion length. This suggests that nanoparticulate OPVs with enhanced exciton diffusion can reach considerably higher efficiencies. Recent demonstrations of high-efficiency small solar cells fabricated using the sequential deposition of electron donor and non-fullerene acceptor layers from green solvents indicate an alternative way for environmentally friendly production.

Large diffusion length is also required for ordered heterojunction nanostructures<sup>66–68</sup> where one material is patterned (donor or acceptor) and the other is added to achieve the desired morphology, as it will allow the nanostructure to be on large length scales. Large diffusion length has two advantages for ordered heterojunctions: the first is that the structure will be easier to make and the other is that larger spacing will make it easier to get one phase to fill the gaps in between features of the others.

In planar heterojunction solar cells the 1D diffusion length defines the thickness of the donor and acceptor layers to be used. To absorb the incident light efficiently in a bilayer, the combined donor and acceptor layer thicknesses should be around 100 nm. To accomplish this, a 1D diffusion length of at least 50 nm will be required in each material. The optimized 1D diffusion length in OPV materials is ~20 nm (Table 1) and limits the efficiency of solar cells made using a bilayer. Further increase in exciton transport distance is necessary to make bilayer technology attractive for solar cell applications, possibly by combining long  $L_D$  with layer-to-layer FRET or energy cascade. This potentially can lead to simpler and more consistent device fabrication as compared with a BHJ. Also, the problems of charge recombination could be better tackled in such structures.

We next briefly consider strategies that could further increase exciton diffusion. Recently, long-range energy transport over 200 nm and more has been reported in self-organized organic nanofibers at room temperature.<sup>69,70</sup> This is substantially longer than predicted by the self-Förster radius calculations for the point dipoles. The authors suggested that some degree of intermolecular electronic coherence increases the mean exciton hopping range and helps them to diffuse further. Albeit not yet applied in OPVs, these findings suggest that high structural order in nanofibers can support long-range exciton diffusion at room temperature and are very relevant to the development of new photovoltaic materials.

Because singlet exciton diffusion occurs by Förster energy transfer between molecules, it should be possible to increase the diffusivity by enhancing the local photonic mode density using optical microcavities or other optical confinement.<sup>71</sup> This is an example of weak exciton-photon coupling. In optically confined systems it is also possible to achieve strong exciton-photon coupling and to create new quasiparticles known as polaritons. The effective mass of a polariton is a weighted average of the exciton and photon components; hence, polariton wavefunctions can be delocalized over many lattice constants or molecules. This can enable long-range polariton diffusion in the plane of a microcavity where the optical field is strongest. In a high Q microcavity with GaAs quantum wells, polaritons have been reported to travel a distance of 1 mm.<sup>72</sup> Cryogenic temperatures are necessary to achieve strong exciton-photon coupling in inorganic quantum wells because of the weak exciton binding energy of inorganic semiconductors. In contrast, the large exciton binding energy in organic semiconductors enables polariton formation at room temperature and low-threshold polariton lasing in microcavities with substantially lower Q factors than inorganic quantum wells.<sup>73</sup> There are several reports showing that energy transfer can occur over a distance of 60–100 nm between dye molecules separated by a spacer layer in planar microcavities, which is much larger than that permitted by Förster energy transfer.<sup>74,75</sup> This suggests that polariton-assisted energy transport can occur in organic semiconductors over a distance comparable with the light absorption depth (~100 nm). This would enable efficient harvesting of excitons using planar heterojunctions with patterned structures. Obviously, the spectral range of resonant microcavity modes is limited, so this approach is likely

to be more suitable in narrowband OPVs for indoor light harvesting or photodetectors. In addition, strong exciton-photon coupling can red-shift the absorption edge and help to harvest lower-energy photons while preserving the open-circuit voltage value.<sup>76</sup>

In summary, recent studies have shown that 3D exciton diffusion length in thin films of organic semiconductors can be increased beyond 40 nm by processing. This enables the use of larger donor and acceptor domain sizes in BHJs, which improve charge pair dissociation and extraction efficiencies. Longer exciton diffusion can boost the efficiencies of nanoparticulate OPVs, which offer environmentally friendly low-cost production by ink-jet printing or sputtering from solutions of electron donor and acceptor nanoparticles. It also opens new opportunities to optimize the active layer morphology by sequential deposition of donor and acceptor layers. Further developments of highly ordered self-organized systems that can support long-range exciton diffusion length in combination with polariton-assisted energy transfer can make planar heterojunctions a viable approach to OPVs.

## ACKNOWLEDGMENTS

We acknowledge support from the European Research Council (grant 321305). We are also grateful to EPSRC for support from grants (EP/L017008/1) and (EP/M025330/1).

## AUTHOR CONTRIBUTIONS

The paper was written by all three authors.

## DECLARATION OF INTERESTS

The authors confirm there are no competing interests.

## REFERENCES

- World's largest BIOPV installation on a roof – France. <https://www.heliatek.com/projects/biopv-la-rochelle/>.
- Krebs, F.C. (2009). Roll-to-roll fabrication of monolithic large-area polymer solar cells free from indium-tin-oxide. *Sol. Energy Mater. Sol. Cells*. 93, 1636–1641.
- Sariciftci, N.S., Smilowitz, L., Heeger, A.J., and Wudl, F. (1992). Photoinduced electron transfer from a conducting polymer to buckminsterfullerene. *Science* 258, 1474–1476.
- Menke, S.M., and Holmes, R.J. (2014). Exciton diffusion in organic photovoltaic cells. *Energy Environ. Sci.* 7, 499–512.
- Mikhnenko, O.V., Blom, P.W., and Nguyen, T.-Q. (2015). Exciton diffusion in organic semiconductors. *Energy Environ. Sci.* 8, 1867–1888.
- Tamai, Y., Ohkita, H., Bente, H., and Ito, S. (2015). Exciton diffusion in conjugated polymers: from fundamental understanding to improvement in photovoltaic conversion efficiency. *J. Phys. Chem. Lett.* 6, 3417–3428.
- G Hedley, G.J., Ruseckas, A., and Samuel, I.D.W. (2017). Light harvesting for organic photovoltaics. *Chem. Rev.* 117, 796–837.
- Zhang, Y., Sajjad, M.T., Blaszczyk, O., Parnell, A.J., Ruseckas, A., Serrano, L.A., Cooke, G., and Samuel, I.D.W. (2019). Large crystalline domains and enhanced exciton diffusion length enable efficient organic solar cells. *Chem. Mater.* 31, 6548–6557.
- Zhang, Y., Sajjad, M.T., Blaszczyk, O., Ruseckas, A., Serrano, L.A., Cooke, G., and Samuel, I.D.W. (2019). Enhanced exciton harvesting in a planar heterojunction organic photovoltaic device by solvent vapor annealing. *Org. Electron.* 70, 162–166.
- Luppi, B.T., Majak, D., Gupta, M., Rivard, E., and Shankar, K. (2019). Triplet excitons: improving exciton diffusion length for enhanced organic photovoltaics. *J. Mater. Chem. A* 7, 2445–2463.
- Cui, Y., Yao, H., Zhang, J., Zhang, T., Wang, Y., Hong, L., Xian, K., Xu, B., Zhang, S., Peng, J., et al. (2019). Over 16% efficiency organic photovoltaic cells enabled by a chlorinated acceptor with increased open-circuit voltages. *Nat. Commun.* 10, 2515.
- Lin, Y., Adilbekova, B., Firdaus, Y., Yengel, E., Faber, H., Sajjad, M., Zheng, X., Yarali, E., Seithkan, A., Bakr, O.M., et al. (2019). 17% efficient organic solar cells based on liquid exfoliated WS<sub>2</sub> as a replacement for PEDOT: PSS. *Adv. Mater.* 15, 1902965.
- Holmes, N.P., Marks, M., Kumar, P., Kroon, R., Barr, M.G., Nicolaidis, N., Feron, K., Pivrikas, A., Fahy, A., de Zerio Mendaza, A.D., et al. (2016). Nano-pathways: bridging the divide between water-processable nanoparticulate and bulk heterojunction organic photovoltaics. *Nano Energy* 19, 495–510.
- Holmes, N.P., Nicolaidis, N., Feron, K., Barr, M., Burke, K.B., Al-Mudhaffer, M., Sista, P., Kilcoyne, A.D., Stefan, M.C., Zhou, X., et al. (2015). Probing the origin of photocurrent in nanoparticulate organic photovoltaics. *Solar Sol. Energy Mater. Sol. Cells* 140, 412–421.
- Al-Mudhaffer, M.F., Griffith, M.J., Feron, K., Nicolaidis, N.C., Cooling, N.A., Zhou, X., Holdsworth, J., Belcher, W.J., and Dastoor, P.C. (2018). The origin of performance limitations in miniemulsion nanoparticulate organic photovoltaic devices. *Sol. Energy Mater. Sol. Cells* 175, 77–88.
- Shaw, P.E., Ruseckas, A., and Samuel, I.D.W. (2008). Exciton diffusion measurements in poly (3-hexylthiophene). *Adv. Mater.* 20, 3516–3520.
- Scully, S.R., and McGehee, M.D. (2006). Effects of optical interference and energy transfer on exciton diffusion length measurements in organic semiconductors. *J. Appl. Phys.* 100, 034907.
- Markov, D.E., Amsterdam, E., Blom, P.W., Sieval, A.B., and Hummelen, J.C. (2005). Accurate measurement of the exciton diffusion length in a conjugated polymer using a heterostructure with a side-chain cross-linked

- fullerene layer. *J. Phys. Chem. A* **109**, 5266–5274.
19. Long, Y., Hedley, G.J., Ruseckas, A., Chowdhury, M., Roland, T., Serrano, L.A., Cooke, G., and Samuel, I.D.W. (2017). Effect of annealing on exciton diffusion in a high performance small molecule organic photovoltaic material. *ACS Appl. Mater. Inter.* **9**, 14945–14952.
20. Ward, A.J., Ruseckas, A., and Samuel, I.D.W. (2012). A shift from diffusion assisted to energy transfer controlled fluorescence quenching in polymer–fullerene photovoltaic blends. *J. Phys. Chem. C* **116**, 23931–23937.
21. Ward, A.J., Ruseckas, A., Kareem, M.M., Ebenhoch, B., Serrano, L.A., Al-Eid, M., Fitzpatrick, B., Rotello, V.M., Cooke, G., and Samuel, I.D.W. (2015). The impact of driving force on electron transfer rates in photovoltaic donor–acceptor blends. *Adv. Mater.* **27**, 2496–2500.
22. Mulder, B.J. (1967). Diffusion and Surface Reactions of Singlet Excitons in Anthracene (Technische Hogeschool Eindhoven). <https://doi.org/10.6100/IR36174>.
23. Pettersson, L.A., Roman, L.S., and Inganäs, O. (1999). Modeling photocurrent action spectra of photovoltaic devices based on organic thin films. *J. Appl. Phys.* **86**, 487–496.
24. Halls, J., and Friend, R. (1997). The photovoltaic effect in a poly (p-phenylenevinylene)/perylene heterojunction. *Synth. Met.* **85**, 1307–1308.
25. Mullenbach, T.K., Curtin, I.J., Zhang, T., and Holmes, R.J. (2017). Probing dark exciton diffusion using photovoltage. *Nat. Commun.* **8**, 14215.
26. Siegmund, B., Sajjad, M.T., Widmer, J., Ray, D., Koerner, C., Riede, M., Leo, K., Samuel, I.D.W., and Vandewal, K. (2017). Exciton diffusion length and charge extraction yield in organic bilayer solar cells. *Adv. Mater.* **29**, 1604424.
27. Zhang, T., Dement, D.B., Ferry, V.E., and Holmes, R.J. (2019b). Intrinsic measurements of exciton transport in photovoltaic cells. *Nat. Commun.* **10**, 1156.
28. Shi, K., Curtin, I.J., Healy, A.T., Zhang, T., Rai, D., Blank, D.A., and Holmes, R.J. (2020). Probing enhanced exciton diffusion in a triplet-sensitized organic photovoltaic cell. *J. Phys. Chem. C* **124**, 3489–3495.
29. Masri, Z., Ruseckas, A., Emelianova, E.V., Wang, L., Bansal, A.K., Matheson, A., Lemke, H.T., Nielsen, M.M., Nguyen, H., Coulembier, O., et al. (2013). Molecular weight dependence of exciton diffusion in poly (3-hexylthiophene). *Adv. Energy Mater.* **3**, 1445–1453.
30. Chowdhury, M., Sajjad, M.T., Savikhin, V., Hergue, N., Sutija, K., Oosterhout, S., Toney, M.F., Ruseckas, A., and Samuel, I.D.W. (2017). Tuning crystalline ordering by annealing and additives to study its effect on exciton diffusion in a polyalkylthiophene copolymer. *Phys. Chem. Chem. Phys.* **19**, 12441–12451.
31. Sajjad, M.T., Blaszczyk, O., Jagadamma, L.K., Roland, T.J., Chowdhury, M., Ruseckas, A., and Samuel, I.D.W. (2018). Engineered exciton diffusion length enhances device efficiency in small molecule photovoltaics. *J. Mater. Chem. A* **6**, 9445–9450.
32. Sajjad, M.T., Zhang, Y., Geraghty, P.B., Mitchell, V.D., Ruseckas, A., Blaszczyk, O., Jones, D.J., and Samuel, I.D.W. (2019). Tailoring exciton diffusion and domain size in photovoltaic small molecules by processing. *J. Mater. Chem. C* **7**, 7922–7928.
33. Sajjad, M.T., Ward, A.J., Kästner, C., Ruseckas, A., Hoppe, H., and Samuel, I.D.W. (2015). Controlling exciton diffusion and fullerene distribution in photovoltaic blends by side chain modification. *J. Phys. Chem. Lett.* **6**, 3054–3060.
34. Chandrabose, S., Chen, K., Barker, A.J., Sutton, J.J., Prasad, S.K., Zhu, J., Zhou, J., Gordon, K.C., Xie, Z., Zhan, X., and Hodgkiss, J.M. (2019). High exciton diffusion coefficients in fused ring electron acceptor films. *J. Am. Chem. Soc.* **141**, 6922–6929.
35. Kersting, R., Lemmer, U., Mahrt, R., Leo, K., Kurz, H., Bässler, H., and Göbel, E. (1993). Femtosecond energy relaxation in  $\pi$ -conjugated polymers. *Phys. Rev. Lett.* **70**, 3820.
36. Mollay, B., Lemmer, U., Kersting, R., Mahrt, R., Kurz, H., Kauffmann, H., and Bässler, H. (1994). Dynamics of singlet excitations in conjugated polymers: poly (phenylenevinylene) and poly (phenylphenylenevinylene). *Phys. Rev. B* **50**, 10769.
37. Hayes, G., Samuel, I.D.W., and Phillips, R. (1995). Exciton dynamics in electroluminescent polymers studied by femtosecond time-resolved photoluminescence spectroscopy. *Phys. Rev. B* **52**, 11569–11572.
38. Ruseckas, A., Theander, M., Valkunas, L., Andersson, M., Inganäs, O., and Sundström, V. (1998). Energy transfer in a conjugated polymer with reduced inter-chain coupling. *J. Lumin.* **76–77**, 474–477.
39. Meskers, S.C., Hübner, J., Oestreich, M., and Bässler, H. (2001). Dispersive relaxation dynamics of photoexcitations in a polyfluorene film involving energy transfer: experiment and Monte Carlo simulations. *J. Phys. Chem. B* **105**, 9139–9149.
40. Denis, J.-C., Schumacher, S., Hedley, G.J., Ruseckas, A., Morawski, P.O., Wang, Y., Allard, S., Scherf, U., Turnbull, G.A., and Samuel, I.D.W. (2015). Subpicosecond exciton dynamics in polyfluorene films from experiment and microscopic theory. *J. Phys. Chem. C* **119**, 9734–9744.
41. Movaghar, B., Grünewald, M., Ries, B., Bässler, H., and Würtz, D. (1986). Diffusion and relaxation of energy in disordered organic and inorganic materials. *Phys. Rev. B* **33**, 5545.
42. Laquai, F., Park, Y.S., Kim, J.J., and Basché, T. (2009). Excitation energy transfer in organic materials: from fundamentals to optoelectronic devices. *Macromol. Rapid Commun.* **30**, 1203–1231.
43. Lunt, R.R., Benziger, J.B., and Forrest, S.R. (2010). Relationship between crystalline order and exciton diffusion length in molecular organic semiconductors. *Adv. Mater.* **22**, 1233–1236.
44. Lin, J.D., Mikhnenko, O.V., Chen, J., Masri, Z., Ruseckas, A., Mikhailovsky, A., Raab, R.P., Liu, J., Blom, P.W., Loi, M.A., et al. (2014). Systematic study of exciton diffusion length in organic semiconductors by six experimental methods. *Mater. Horiz.* **1**, 280–285.
45. Li, Z., Zhang, X., Woellner, C.F., and Lu, G. (2014). Understanding molecular structure dependence of exciton diffusion in conjugated small molecules. *Appl. Phys. Lett.* **104**, 143303.
46. Sim, M., Shin, J., Shim, C., Kim, M., Jo, S.B., Kim, J.-H., and Cho, K. (2014). Dependence of Exciton diffusion length on crystalline order in conjugated polymers. *J. Phys. Chem. C* **118**, 760–766.
47. Wei, G., Lunt, R.R., Sun, K., Wang, S., Thompson, M.E., and Forrest, S.R. (2010). Efficient, ordered bulk heterojunction nanocrystalline solar cells by annealing of ultrathin squarelike thin films. *Nano Lett.* **10**, 3555–3559.
48. Scully, S.R., Armstrong, P.B., Edder, C., Fréchet, J.M., and McGehee, M.D. (2007). Long-range resonant energy transfer for enhanced exciton harvesting for organic solar cells. *Adv. Mater.* **19**, 2961–2966.
49. Shaw, P.E., Ruseckas, A., and Samuel, I.D.W. (2008a). Distance dependence of excitation energy transfer between spacer-separated conjugated polymer films. *Phys. Rev. B* **78**, 245201.
50. Cnops, K., Rand, B.P., Cheyns, D., Verreert, B., Empl, M.A., and Heremans, P. (2014). 8.4% efficient fullerene-free organic solar cells exploiting long-range exciton energy transfer. *Nat. Commun.* **5**, 3406.
51. Wang, Y., Ohkita, H., Bente, H., and Ito, S. (2015). Efficient exciton harvesting through long-range energy transfer. *ChemPhysChem* **16**, 1263–1267.
52. Honda, S., Ohkita, H., Bente, H., and Ito, S. (2011). Selective dye loading at the heterojunction in polymer/fullerene solar cells. *Adv. Energy Mater.* **1**, 588–598.
53. Reid, O.G., and Rumbles, G. (2016). Resonance energy transfer enables efficient planar heterojunction organic solar cells. *J. Phys. Chem. C* **120**, 87–97.
54. Menke, S.M., Luhman, W.A., and Holmes, R.J. (2013). Tailored exciton diffusion in organic photovoltaic cells for enhanced power conversion efficiency. *Nat. Mater.* **12**, 152–157.
55. Caplins, B.W., Mullenbach, T.K., Holmes, R.J., and Blank, D.A. (2015). Intermolecular interactions determine exciton lifetimes in neat films and solid state solutions of metal-free phthalocyanine. *J. Phys. Chem. C* **119**, 27340–27347.
56. Hou, J., Inganäs, O., Friend, R.H., and Gao, F. (2018). Organic solar cells based on non-fullerene acceptors. *Nat. Mater.* **17**, 119–128.
57. J Yuan, J., Zhang, Y., Zhou, L., Zhang, G., Yip, H.-L., Lau, T.-K., Lu, X., Zhu, C., Peng, H., Johnson, P.A., et al. (2019). Single-junction organic solar cell with over 15% efficiency using fused-ring acceptor with electron-deficient core. *Joule* **3**, 1140–1151.
58. Jagadamma, L.K., Taylor, R.G., Kanibolotsky, A.L., Sajjad, M.T., Wright, I.A., Horton, P.N., Coles, S.J., Samuel, I.D.W., and Skabara, P.J. (2019). Highly efficient fullerene and non-fullerene based ternary organic solar cells

incorporating a new tetrathioic-cored semiconductor. *Sustain. Energy Fuels* 3, 2087–2099.

59. Lin, Y., Zhao, F., Prasad, S.K., Chen, J.D., Cai, W., Zhang, Q., Chen, K., Wu, Y., Ma, W., Gao, F., et al. (2018). Balanced partnership between donor and acceptor components in nonfullerene organic solar cells with >12% efficiency. *Adv. Mater.* 30, 1706363.
60. Cheng, P., Hou, J., Li, Y., and Zhan, X. (2014). layer-by-layer solution-processed low-bandgap polymer-PC61BM solar cells with high efficiency. *Adv. Energy Mater.* 4, 1301349.
61. Aguirre, J.C., Hawks, S.A., Ferreira, A.S., Yee, P., Subramaniyan, S., Jenekhe, S.A., Tolbert, S.H., and Schwartz, B.J. (2015). Sequential processing for organic photovoltaics: design rules for morphology control by tailored semi-orthogonal solvent blends. *Adv. Energy Mater.* 5, 1402020.
62. Sun, R., Guo, J., Wu, Q., Zhang, Z., Yang, W., Guo, J., Shi, M., Zhang, Y., Kahmann, S., Ye, L., et al. (2019). A multi-objective optimization-based layer-by-layer blade-coating approach for organic solar cells: rational control of vertical stratification for high performance. *Energy Environ. Sci.* 12, 3118–3132.
63. Dong, S., Zhang, K., Xie, B., Xiao, J., Yip, H.L., Yan, H., Huang, F., and Cao, Y. (2019). High-performance large-area organic solar cells enabled by sequential bilayer processing via nonhalogenated solvents. *Adv. Energy Mater.* 9, 1802832.
64. Ye, L., Xiong, Y., Chen, Z., Zhang, Q., Fei, Z., Henry, R., Heeney, M., O'Connor, B.T., You, W., and Ade, H. (2019). Sequential deposition of organic films with eco-compatible solvents improves performance and enables over 12%-efficiency nonfullerene solar cells. *Adv. Mater.* 31, 1808153.
65. Zhang, J., Futscher, M.H., Lami, V., Kosasih, F.U., Cho, C., Gu, Q., Sadhanala, A., Pearson, A.J., Kan, B., Divitini, G., et al. (2019a). Sequentially deposited versus conventional nonfullerene organic solar cells: interfacial trap states, vertical stratification, and exciton dissociation. *Adv. Energy Mater.* 9, 1902145.
66. Matsuo, Y., Sato, Y., Niinomi, T., Soga, I., Tanaka, H., and Nakamura, E. (2009). Columnar structure in bulk heterojunction in solution-processable three-layered pin organic photovoltaic devices using tetrabenzoporphyrin precursor and silylmethyl [60] fullerene. *J. Am. Chem. Soc.* 131, 16048–16050.
67. He, X., Gao, F., Tu, G., Hasko, D., Huttner, S., Steiner, U., Greenham, N.C., Friend, R.H., and Huck, W.T. (2010). Formation of nanopatterned polymer blends in photovoltaic devices. *Nano Lett.* 10, 1302–1307.
68. J Kim, J.S., Park, Y., Lee, D.Y., Lee, J.H., Park, J.H., Kim, J.K., and Cho, K. (2010). Poly (3-hexylthiophene) nanorods with aligned chain orientation for organic photovoltaics. *Adv. Funct. Mater.* 20, 540–545.
69. Jin, X.-H., Price, M.B., Finnegan, J.R., Boott, C.E., Richter, J.M., Rao, A., Menke, S.M., Friend, R.H., Whittell, G.R., and Manners, I. (2018). Long-range exciton transport in conjugated polymer nanofibers prepared by seeded growth. *Science* 360, 897–900.
70. Haedler, A.T., Kreger, K., Issac, A., Wittmann, B., Kivala, M., Hammer, N., Kohler, J., Schmidt, H.-W., and Hildner, R. (2015). Long-range energy transport in single supramolecular nanofibres at room temperature. *Nature* 523, 196–199.
71. Andrew, P., and Barnes, W.L. (2000). Förster energy transfer in an optical microcavity. *Science* 290, 785–788.
72. Steger, M., Liu, G., Nelsen, B., Gautham, C., Snoko, D.W., Balili, R., Pfeiffer, L., and West, K. (2013). Long-range ballistic motion and coherent flow of long-lifetime polaritons. *Phys. Rev. B* 88, 235314.
73. Rajendran, S.K., Wei, M., Ohadi, H., Ruseckas, A., Turnbull, G.A., and Samuel, I.D.W. (2019). Low threshold polariton lasing from a solution-processed organic semiconductor in a planar microcavity. *Adv. Opt. Mater.* 7, 1801791.
74. Zhong, X., Chervy, T., Zhang, L., Thomas, A., George, J., Genet, C., Hutchison, J.A., and Ebbesen, T.W. (2017). Energy transfer between spatially separated entangled molecules. *Angew. Chem. Int. Ed.* 56, 9034–9038.
75. Georgiou, K., Michetti, P., Gai, L., Cavazzini, M., Shen, Z., and Lidzey, D.G. (2018). Control over energy transfer between fluorescent BODIPY dyes in a strongly coupled microcavity. *ACS Photon.* 5, 258–266.
76. Nikolis, V.C., Mischok, A., Siegmund, B., Kublitski, J., Jia, X., Benduhn, J., Hörmann, U., Neher, D., Gather, M.C., Spoltore, D., and Vandewal, K. (2019). Strong light-matter coupling for reduced photon energy losses in organic photovoltaics. *Nat. Commun.* 10, 3706.